Algorithms for the Transient Simulation of Lossy Interconnect

Jaijeet S. Roychowdhury, A. Richard Newton, *Fellow, IEEE,* and Donald O. Pederson, *Life Fellow, IEEE*

***Abstract*— In this paper, a new linear-time technique is described for the simulation of lossy lines with frequency-independent R, L, C and G. Exact analytic forms are shown to exist for the frequency-independent lossy line, with application in both the new technique and the conventional convolution method. Numerical convolution formulae that exploit the analytic forms are presented. Experimental results for industrial circuits indicate that the new technique can be 10 and 50 times faster than the convolution and lumped-RLC methods, respectively, for long simulations.**

I. Introduction

THE PROBLEM of simulating lossy transmission lines within nonlinear circuits has recently come into prominence, in large part due to the increasing importance of multi-chip modules (MCM's) in state-of-the-art high-performance designs. At the high speeds of MCM's, chip-to-chip interconnections behave as lossy transmission lines, effects due to which can seriously impair signal quality. Accurate and efficient simulation techniques are needed during design and verification to ensure that transmission line effects do not affect correct operation.

In this work, a new technique featuring linear time-complexity is presented for the simulation of lossy transmission lines with electrical parameters (R, L, C, G) invariant with frequency[1] ("simple lossy" lines). Exact analytic forms for impulse responses and related functions are given, with application in the new technique as well as in conventional convolution (described later in this section). Formulae which are especially suited for numerical convolution with these analytic forms are developed. Experimental results for industrial circuits and interconnect confirm the linear complexity of the new method and indicate significant speed advantage over the convolution and lumped-RLC methods.

Many techniques exist for the simulation of lossy transmission lines. Simulation in the frequency domain is especially convenient for entirely linear circuits [1], [2] and is also possible by using the waveform relaxation methodology [3], [4] coupled with numerical Fourier techniques [5]–[7]. In the time domain, segmentation using lumped R, L, C and G elements to represent each segment (the "lumped-RLC" method) [8] is widely used. A variant in which individual segments are represented by a lossless line and lumped loss elements has also been proposed [9]. Padé approximation in the form of Asymptotic Waveform Evaluation (AWE) [10], [11] has been applied to lossy line simulation by several authors [12]–[14]. An optimization-based approach for determining a reduced-order model has been proposed [15].

Simulation based on time-domain convolution with the impulse responses of the lossy line has been proposed by several authors [16], [17]. A limitation of convolution is that the computation required increases as the square of the number of time-points in the simulation ("quadratic complexity"). The impulse responses of the lossy line have been determined by numerical inversion of frequency-domain formulae in the previous work on convolution.

For most lossy line simulations today, the constant-parameter simple lossy line model is adequate [18], but in very high-speed applications, it may be necessary to model R, L, C and G as varying with frequency ("frequency-varying" models) to account for skin effect, dielectric dispersion and other high-frequency physical phenomena. The techniques presented in this paper exploit properties of the simple lossy line and are not applicable to frequency-varying models.

The new technique achieves linear complexity by utilizing the internal state of the line, and for this reason is referred to as the *state-based technique*. The internal state of the line is captured as a spatial distribution of instantaneous voltages and currents, which are sampled at appropriate locations throughout the line. A feature of particular note about the new technique is that dynamic variation of these sample points is possible from time-point to time-point during the simulation (see Section IV for further details). This makes the exploitation of latency convenient.

In Section II, the state-based method and the analytic forms are presented. In Section III, the numerical formulae for convolution are given. Section IV contains an evaluation of the state-based method with reference to the convolution and lumped-RLC methods, while Section V deals with implementation issues. In Section VI, experimental results are presented.

II. State-Based Technique

The development of the state-based method starts from the Telegrapher Equations [17], partial differential equations in

Manuscript received April 1, 1992. This work was supported by AT&T Bell Laboratories, Raytheon, and the California MICRO Program. This paper was recommended by Associate Editor J. White.

J. S. Roychowdhury was with the Dept. of Electrical Engineering and Computer Sciences at the University of California at Berkeley. He is now with AT&T Bell Laboratories, Allentown, PA 18103.

A. R. Newton and D. O. Pederson are with the Dept. of Electrical Engineering and Computer Sciences at the University of California at Berkeley, Berkeley, CA 94720.

IEEE Log Number 9212369.

[1] i.e., not applicable to "frequency-varying" models (described later in this section).

time and space that describe the transient behaviour of the lossy line:

$$\frac{\partial v}{\partial x} = -\left(L\frac{\partial i}{\partial t} + Ri\right) \tag{1}$$

$$\frac{\partial i}{\partial x} = -\left(C\frac{\partial v}{\partial t} + Gv\right) \tag{2}$$

The above hold for x varying between 0 and l (the length of the transmission line). $v(x,t)$ and $i(x,t)$ are the voltage and current at the point x in the line at time t, respectively. Without loss of generality (because (1) and (2) are time-invariant), it is assumed that the simulation starts from time 0.

The inputs to the transmission line are the port variables $v_1(t) = v(0,t)$, $i_1(t) = i(0,t)$, $v_2(t) = v(l,t)$ and $i_2(t) = -i(l,t)$. These four port variables specify the *boundary conditions* of (1) and (2).

In addition to the boundary conditions which represent the inputs to the line from the external circuit, the internal state of the transmission line also determines the future behaviour of the line. This internal state is stored in the energy-storing distributed inductance and capacitance and is specified by the voltages and currents in the line's interior at time 0: $v_0(x) = v(x,0)$ and $i_0(x) = i(x,0)$, the *initial conditions* for (1) and (2). The combination of the Telegrapher Equations and the boundary and initial conditions specify the future behaviour of the line uniquely.

While similar to D'Alembert's procedure [19] for solving the wave equation, the following derivation contains several differences that lead to analytic forms and the state-based method. Laplace transforms are taken (in t) of (1) and (2) to arrive at ordinary differential equations in x and s, the Laplace variable:

$$\frac{\partial V}{\partial x} = -(sL + R)I + Li_0(x) \tag{3}$$

$$\frac{\partial I}{\partial x} = -(sC + G)V + Cv_0(x) \tag{4}$$

V and I refer to $V(x,s)$ and $I(x,s)$, the Laplace transformed variables.

To uncouple the above equations, a basis change is performed from the variables V and I to new ("scattering parameter") variables p and q, defined as follows:

$$p(x,s) = \frac{V(x,s) + Z(s)I(x,s)}{2} \tag{5}$$

$$q(x,s) = \frac{V(x,s) - Z(s)I(x,s)}{2} \tag{6}$$

$Z(s)$ is the frequency domain characteristic impedance of the line:

$$Z(s) = \sqrt{\frac{sL + R}{sC + G}} \tag{7}$$

Equations (5) and (6) are rewritten to express V and I in terms of p and q; using these, (3) and (4) are rewritten in terms of p and q. Two decoupled linear first-order ODEs in x are obtained by adding and subtracting (3) and (4):

$$\frac{\partial p}{\partial x} + \lambda(s)p = \frac{Li_0(x) + Z(s)Cv_0(x)}{2} \tag{8}$$

$$\frac{\partial q}{\partial x} - \lambda(s)q = \frac{Li_0(x) - Z(s)Cv_0(x)}{2} \tag{9}$$

$\lambda(s)$ is the frequency-domain propagation constant of the line:

$$\lambda(s) = \sqrt{(sC + G)(sL + R)} \tag{10}$$

The general solution of any first-order ordinary differential equation of the type

$$\frac{\partial y}{\partial x} + P(x)y = Q(x) \tag{11}$$

is

$$y = e^{-\int P(x)dx}\left(C_1 + \int Q(x)e^{\int P(y)dy}dx\right) \tag{12}$$

Equation (12) is applied to (8) and (9) to obtain solutions for p and q:

$$p(x,s) = e^{-\lambda x}\left(A + \frac{1}{2}\int_0^x e^{\lambda y}[Li_0(y) + Z(s)Cv_0(y)]dy\right) \tag{13}$$

$$q(x,s) = e^{\lambda x}\left(B + \frac{1}{2}\int_0^x e^{-\lambda y}[Li_0(y) - Z(s)Cv_0(y)]dy\right) \tag{14}$$

The boundary condition at $x = 0$ is applied to (13), and that at $x = l$ to (14), to determine the constants A and B which are substituted for to obtain

$$p(x,s) - e^{-\lambda x}p(0,s) = \int_0^x \frac{e^{-\lambda(x-y)}}{2}[Li_0(y) + Z(s)Cv_0(y)]dy \tag{15}$$

$$q(l,s)e^{-\lambda(l-x)} - q(x,s) = \int_x^l \frac{e^{-\lambda(y-x)}}{2}[Li_0(y) - Z(s)Cv_0(y)]dy \tag{16}$$

Now p and q are substituted for in terms of V and I (using (5) and (7)) and the resulting equations divided by $Z(s)$ to obtain

$$[V(x,s)Y(s) + I(x,s)] - e^{-\lambda x}[V(0,s)Y(s) + I(0,s)] = \int_0^x e^{-\lambda(x-y)}[Li_0(y)Y(s) + Cv_0(y)]dy \tag{17}$$

$$[V(l,s)Y(s) - I(l,s)]e^{-\lambda(l-x)} - [V(x,s)Y(s) - I(x,s)] = \int_x^l e^{-\lambda(y-x)}[Li_0(y)Y(s) - Cv_0(y)]dy \tag{18}$$

where

$$Y(s) = \frac{1}{Z(s)} = \sqrt{\frac{sC + G}{sL + R}} \tag{19}$$

Equations (17) and (18) need to be Laplace inverted to obtain time-domain equations. In doing so, however, it is important to note that the Laplace inversion operator cannot be transmitted into the space integrals on the RHS of the

equations, because the integrands are not uniformly continuous (this may be verified easily for the lossless case with $v_0(\cdot)$ and $i_0(\cdot)$ constant). Therefore, before the Laplace inversion operator is applied, the space integrals are evaluated in the frequency domain by making the assumption that $v_0(\cdot)$ and $i_0(\cdot)$ are piecewise constant functions (formulae for the piecewise linear case, as well as for the general case of any piecewise continuous $v_0(\cdot)$ and $i_0(\cdot)$, are available, but are omitted for brevity). The interval $[0,l]$ is partitioned into a number of segments between the points $x_0, x_1, \ldots, x_{n_l}$, with $x_0 = 0$ and $x_{n_l} = l$[2]. Over each interval $I_j = [x_{j-1}, x_j]$, the piecewise constant assumption about the initial states is applied; $v_0(x)$ and $i_0(x)$ are replaced by the constants v_{0j} and i_{0j}. Define the index n_y by the relation $x_{n_y} = y$ for any $y \in \{x_1, \ldots, x_{n_l}\}$, with $n_0 = 1$. The integrals on the RHS of (17) and (18) are split into a sum of integrals, each over I_j; the integrand in each of these integrals is simply an exponential which is easily integrated to yield

$$\begin{aligned}&[Y_0V(x,s)H_Y(s)+I(x,s)]-[Y_0V(0,s)H_{\gamma Y}(x,s)\\&+I(0,s)H_\gamma(x,s)]\\&=\sum_{j=1}^{n_x}\left\{\begin{matrix} i_{0j}[h_{S\gamma Y}(x-x_j,s)-H_{S\gamma Y}(x-x_{j-1},s)]\\ +Y_0v_{0j}[H_{S\gamma}(x-x_j,s)-H_{S\gamma}(x-x_{j-1},s)]\end{matrix}\right\} \quad (20)\\&[Y_0V(l,s)H_{\gamma Y}(l-x,s)-I(l,s)H_\gamma(l-x,s)]\\&-[Y_0V(x,s)H_Y(s)-I(x,s)]\\&=\sum_{j=n_x}^{n_l}\left\{\begin{matrix} i_{0j}[H_{S\gamma Y}(x_{j-1}-x,s)-H_{S\gamma Y}(x_j-x,s)]\\ -Y_0v_{0j}[H_{S\gamma}(x_{j-1}-x,s)-H_{S\gamma}(x_j-x,s)]\end{matrix}\right\} \quad (21)\end{aligned}$$

where

$$Y_0=\sqrt{\frac{C}{L}},\quad H_Y(s)=\frac{Y(s)}{Y_0},H_\gamma(x,s)=e^{-\lambda(s)x} \quad (22)$$

$$H_{\gamma Y}(x,s)=H_Y(s)H_\gamma(x,s),H_{S\gamma Y}(x,s)=LY(s)\frac{e^{-\lambda(s)x}}{\lambda(s)} \quad (23)$$

$$H_{S\gamma}(x,s)=\sqrt{LC}\,\frac{e^{-\lambda(s)x}}{\lambda(s)} \quad (24)$$

Let h_Y, $h_{\gamma Y}$, h_γ, $h_{S\gamma Y}$ and $h_{S\gamma}$ denote the inverse Laplace transforms of H_Y, $H_{\gamma Y}$, H_γ, $H_{S\gamma Y}$ and $H_{S\gamma}$ respectively. Define

$$\gamma_0=\sqrt{LC},\quad \beta=\frac{1}{2}\left(\frac{R}{L}+\frac{G}{C}\right),\quad \alpha=\frac{1}{2}\left(\frac{R}{L}-\frac{G}{C}\right) \quad (25)$$

and note that

$$H_Y(s)=\frac{1}{Y_0}\sqrt{\frac{sC+G}{sL+R}}=\sqrt{\frac{(s+\beta)-\alpha}{(s+\beta)+\alpha}} \quad (26)$$

$$H_\gamma(x,s)=e^{-x\sqrt{sC(sL+R)}}=e^{-\gamma_0x\sqrt{(s+\beta)^2-\alpha^2}} \quad (27)$$

$$H_{\gamma Y}(x,s)=H_Y(x,s)H_\gamma(x,s) \quad (28)$$

$$H_{S\gamma}(x,s)=\frac{e^{-\gamma_0x\sqrt{(s+\beta)^2-\alpha^2}}}{\sqrt{(s+\beta)^2-\alpha^2}} \quad (29)$$

[2] In Section V, a scheme for selecting these points dynamically is described.

TABLE I
LAPLACE TRANSFORM PAIRS (FODOR [20])

No.	$F(s)$	$f(t)$
1	$\frac{1}{\sqrt{s^2-\alpha^2}}e^{-T\sqrt{s^2-\alpha^2}}$	$1(t-T)I_0\left(\alpha\sqrt{t^2-T^2}\right)$
2	$e^{-T\sqrt{s^2-\alpha^2}}-e^{-sT}$	$1(t-T)\frac{\alpha T}{\sqrt{t^2-T^2}}I_1\left(\alpha\sqrt{t^2-T^2}\right)$
3	$\frac{1}{\sqrt{s^2-\alpha^2}}$	$I_0(\alpha t)$
4	$\frac{\sqrt{s+\alpha}}{\sqrt{s-\alpha}}-1$	$\alpha[I_0(\alpha t)+I_1(\alpha t)]$
5	$\sqrt{s+\alpha}-\sqrt{s+\beta}$	$\frac{1}{2\sqrt{\pi t^3}}[e^{-\beta t}-e^{-\alpha t}]$

$$H_{S\gamma Y}(x,s)=\frac{e^{-\gamma_0x\sqrt{(s+\beta)^2-\alpha^2}}}{(s+\beta)+\alpha} \quad (30)$$

Using Table I, the relation[3] $I_0' = I_1$ and elementary properties of the Laplace transform, the following expressions are obtained for $h_Y(t)$, $h_\gamma(x,t)$, $h_{\gamma Y}(x,t)$, $h_{S\gamma}(x,t)$ and $h_{S\gamma Y}(x,t)$:

$$h_Y(t)=[\delta(t)+\alpha\{I_1(\alpha t)-I_0(\alpha t)\}]e^{-\beta t} \quad (31)$$

$$h_\gamma(x,t)=\left[\delta(t-\gamma_0x)+u(t-\gamma_0x)\frac{\alpha\gamma_0xI_1\left(\alpha\sqrt{t^2-(\gamma_0x)^2}\right)}{\sqrt{t^2-(\gamma_0x)^2}}\right]e^{-\beta t} \quad (32)$$

$$h_{\gamma Y}(x,t)=\left[\delta(t-\gamma_0x)+u(t-\gamma_0x)\alpha\left\{\frac{tI_1\left(\alpha\sqrt{t^2-(\gamma_0x)^2}\right)}{\sqrt{t^2-(\gamma_0x)^2}}-I_0\left(\alpha\sqrt{t^2-(\gamma_0x)^2}\right)\right\}\right]e^{-\beta t} \quad (33)$$

$$h_{S\gamma}(x,t)=u(t-\gamma_0x)I_0\left(\alpha\sqrt{t^2-(\gamma_0x)^2}\right)e^{-\beta t} \quad (34)$$

$$h_{S\gamma Y}(x,t)=u(t-\gamma_0x)\left[e^{-\alpha(t-\gamma_0x)}+\alpha\gamma_0x\int_{\gamma_0x}^{t}e^{-\alpha(t-\tau)}\frac{I_1\left(\alpha\sqrt{\tau^2-(\gamma_0x)^2}\right)}{\sqrt{\tau^2-(\gamma_0x)^2}}d\tau\right]e^{-\beta t} \quad (35)$$

In the above, $u(\cdot)$ and $\delta(\cdot)$ denote the unit step and delta functions, respectively.

Laplace inversion of (20) and (21) yields the time-domain constitutive relations of the lossy transmission line at any x. Using $*$ to denote convolution (described in Section III), the

[3] I_k is the *modified Bessel function* of k^{th} order.

following time-domain equations are obtained:

$$\begin{aligned}&[Y_0 v(x,t) * h_Y(t) + i(x,t)]\\&- [Y_0 v(0,t) * h_{\gamma Y}(x,t) + i(0,t) * h_\gamma(x,t)]\\&= \sum_{j=1}^{n_x} \left\{ \begin{array}{l} i_{0j}[h_{S\gamma Y}(x - x_j, t) - h_{S\gamma Y}(x - x_{j-1}, t)] \\ +Y_0 v_{0j}[h_{S\gamma}(x - x_j, t) - h_{S\gamma}(x - x_{j-1}, t)] \end{array} \right\} \end{aligned} \quad (36)$$

$$\begin{aligned}&[Y_0 v(l,t) * h_{\gamma Y}(l - x, t) - i(l,t) * h_\gamma(l - x, t)]\\&- [Y_0 v(x,t) * h_Y(t) - i(x,t)]\\&= \sum_{j=n_x}^{n_l} \left\{ \begin{array}{l} i_{0j}[h_{S\gamma Y}(x_{j-1} - x, t) - h_{S\gamma Y}(x_j - x, t)] \\ -Y_0 v_{0j}[h_{S\gamma}(x_{j-1} - x, t) - h_{S\gamma}(x_j - x, t)] \end{array} \right\} \end{aligned} \quad (37)$$

From (36) and (37), the convolution and state-based methods can both be derived. The equations obtained by substituting $x = l$ in (36) and $x = 0$ in (37) are of special interest:

$$\begin{aligned}&[Y_0 v_2(t) * h_Y(t) - i_2(t)]\\&- [Y_0 v_1(t) * h_{\gamma Y}(l,t) + i_1(t) * h_\gamma(l,t)]\\&= \sum_{j=1}^{n_l} \left\{ \begin{array}{l} i_{0j}[h_{S\gamma Y}(l - x_j, t) - h_{S\gamma Y}(l - x_{j-1}, t)] \\ +Y_0 v_{0j}[h_{S\gamma}(l - x_j, t) - h_{S\gamma}(l - x_{j-1}, t)] \end{array} \right\} \end{aligned} \quad (38)$$

$$\begin{aligned}&[Y_0 v_2(t) * h_{\gamma Y}(l,t) + i_2(t) * h_\gamma(l,t)]\\&- [Y_0 v_1(t) * h_Y(t) - i_1(t)]\\&= \sum_{j=1}^{n_l} \left\{ \begin{array}{l} i_{0j}[h_{S\gamma Y}(x_{j-1}, t) - h_{S\gamma Y}(x_j, t)] \\ -Y_0 v_{0j}[h_{S\gamma}(x_{j-1}, t) - h_{S\gamma}(x_j, t)] \end{array} \right\} \end{aligned} \quad (39)$$

The above are the equations of the convolution technique with an arbitrary initial state. It is customary to assume the initial state to be that at a "dc operating point", i.e., a solution of the circuit with no time-variation in any waveform. In such a case, $v_0(x)$ and $i_0(x)$ can be assumed to be zero[4] without loss of generality, and the RHS of (38) and (39) become zero. At time-point t_i in a transient simulation, each convolution on the LHS is carried out from t_0 to t_i, using stored values of v_1, v_2, i_1 and i_2 at t_j for all j, $0 \leq j < i$. The computation required at t_i depends on the index i, leading to the quadratic complexity.

Equations 38 and 39 can be used in another way: at time t_1, the procedure is identical to the convolution method, with convolution over the interval $[t_0, t_1]$, using the initial state of the line at time $t_0 = 0$. The new state of the line at time t_1 is calculated next, using (36) and (37) for each x chosen to sample the internal state. At the next time-point t_2, the newly calculated internal state at t_1 is used as $v_0(x)$ and $i_0(x)$ instead of the original internal state at time t_0, in (36)–(39). In other words, the time-invariance property of the Telegrapher Equations is used, redoing the derivation with initial time t_1.

At time t_2, convolution is performed over only $[t_1, t_2]$, not over $[t_0, t_2]$ as in the conventional convolution method. The internal state of the line at t_1, known from the last time-point, is used to supply the RHS of (38) and (39). The internal state at t_2 is then calculated. This procedure is repeated for every subsequent time-point. The key feature leading to linear time-complexity in this technique is that the computation at time t_i is independent of i, since convolution is always performed over only one interval, $[t_{i-1}, t_i]$. The contribution of the convolution over $[t_0, t_{i-1}]$ is captured by the internal state terms on the RHS, the computation of which is also approximately independent of i.

To solve for the port variables at time t_i, (38) and (39) are used to load the circuit simulator matrix and the right-hand-side vector of excitations. The circuit is then solved by the simulator and the port variables determined at t_i. For each x chosen to sample the new internal state of the line (see Section V), (36) and (37) are then used to obtain the voltage and current at time t_i. It is to be noted that the RHS of these equations depend only on the (known) initial line state, and that $v(x, t_i)$ and $i(x, t_i)$ can be determined from the initial line state and the values of the port variables at the current time-point t_i. In particular, $v(x, t_i)$ and $i(x, t_i)$ at any x are independent of $v(y, t_i)$ and $i(y, t_i)$ for any $y \neq x$; this implies that a system of simultaneous equations does not have to be solved to determine $v(x, t_i)$ and $i(x, t_i)$, the solution being available explicitly.

III. Numerical Convolution

In Section II, the state-based and convolution methods were derived. The computer implementation of both methods calls for the numerical computation of the convolution integral over a period of one or more time-steps. In this section, generalisations of the Backward Euler (BE) and Trapezoidal methods for ODE's suitable for convolution are formulated.

The convolution integral to be calculated is the following:

$$y(t) = \int_0^t x(\tau) h(t - \tau) d\tau \quad (40)$$

In (40), $x(\tau)$ is the input to the linear system, $y(t)$ is the output and $h(\tau)$ is the impulse response (or kernel) of the system. $h(\tau)$ is assumed to be a causal function of time and may be finite or infinite in duration. At any given time t, $x(\tau)$ and $y(\tau)$ are assumed to be known over the half-open interval $[0, t)$[5]. It should be noted that in a circuit context, $x(\tau)$ and $y(\tau)$ are usually also related by a relation other than (40); one may be a function or a causal functional of the other.

In a numerical implementation, $x(t)$ can only be known at a discrete number of points. Knowledge of the values of $x(t)$ at a discrete number of points is not sufficient to specify $y(t)$ uniquely by (40); it is necessary to make assumptions about the overall nature of $x(t)$. In deriving linear multistep methods for differential equations [21], the assumptions that $x(t)$ is piecewise linear and piecewise constant result in the well-known Trapezoidal and Euler methods, respectively. The same assumptions are made here to arrive at generalisations of these methods for convolution.

A. Generalized Trapezoidal Method

If the assumption is made that $x(t)$ is piecewise linear (over the partition $0, t_1, \cdots, t_n$ of $[0, t_n]$), the following numerical

[4] See Appendix B, which deals with the reduction of nonzero dc initial states to zero.

[5] $x(\tau)$ and $y(\tau)$ can be assumed zero for $\tau < 0$ without loss of generality; see Appendix B.

integration formula arises (see Appendix A for the derivation):

$$\int_0^{t_n} x(\tau)h(t_n-\tau)d\tau \approx x_n\frac{F(h,t_n-t_{n-1})}{t_n-t_{n-1}} + \sum_{i=1}^{n-1} x_i\left[\frac{F(h,t_n-t_{i-1})-F(h,t_n-t_i)}{t_i-t_{i-1}} - \frac{F(h,t_n-t_i)-F(h,t_n-t_{i+1})}{t_{i+1}-t_i}\right] \quad (41)$$

In (41), t_i are a discrete set of n timepoints in the interval $[0,t_n]$, with $t_0 = 0$. x_i are samples of $x(\tau)$ at t_i. $F(h,t)$ is defined as follows:

$$F(h,t) \triangleq \int_0^t \int_0^\tau h(\tau')d\tau' d\tau \quad (42)$$

It is to be noted that the first argument of $F(\cdot,\cdot)$ is a function, not a single real number.

If the assumption that $x(t)$ is piecewise-linear is not strictly valid, the integration formula in (41) has an error term. An expression for the error term is given in Appendix A.

B. Generalized Euler Methods

Generalisations of the Backward and Forward Euler methods for numerical convolution can likewise be derived (the derivation is omitted, being similar to and much simpler than that for the Trapezoidal method).

Generalized Backward Euler:

$$\int_0^{t_n} x(\tau)h(t_n-\tau)d\tau \approx x_nE(h,t_n-t_{n-1}) + \sum_{i=1}^{n-1} x_i[E(h,t_n-t_{i-1})-E(h,t_n-t_i)] \quad (43)$$

Generalized Forward Euler:

$$\int_0^{t_n} x(\tau)h(t_n-\tau)d\tau \approx \sum_{i=1}^{n-1} x_i[E(h,t_n-t_{i-1})-E(h,t_n-t_i)] \quad (44)$$

where:

$$E(h,t) \triangleq \int_0^t h(\tau)d\tau \quad (45)$$

C. Analytic Expressions for $E(\cdot,\cdot)$ and $F(\cdot,\cdot)$

One of the advantages of using the above formulae is that analytic expressions for $E(\cdot,\cdot)$ and $F(\cdot,\cdot)$ have been identified for some of the lossy line's impulse responses. The following identities are valid for the special case $\alpha = \beta$ (refer (25)), which holds when G equals zero[6]:

$$\int_0^t h_Y(u)du = e^{-\beta t}I_0(\beta t) \quad (46)$$

$$\int_0^t \int_0^w h_Y(u)du\,dw = te^{-\beta t}\{I_0(\beta t)+I_1(\beta t)\} \quad (47)$$

$$\int_0^t h_{\gamma Y}(x,u)du = 1_{t-\gamma_0 x}e^{-\beta t}I_0\left(\beta\sqrt{t^2-(\gamma_0 x)^2}\right) \quad (48)$$

[6]The $G = 0$ case is useful in many practical applications.

Unfortunately, analytic expressions have not been found so far for $\int_0^t \int_0^w h_{\gamma Y}(x,u)dudw$, $\int_0^t h_\gamma(x,u)du$, and $\int_0^t \int_0^w h_\gamma(x,u)du\,dw$. These are calculated numerically from the impulse responses (see Section V).

IV. Comments

While the segmenting approaches also essentially use the internal state of the line, there are three important differences between them and the state-based method. First, analytic solutions are utilized in the state-based method, leading to improved accuracy. Second, dynamic variation of the locations of the internal state sample points is possible. The points may be spaced densely in regions where waveforms are fast varying, and sparsely in regions where waveforms vary slowly. This leads to the possibility of automatically exploiting latency in "quiet" sections of a circuit, for having few sample points leads to reduced computation. Dynamic variation is impossible in the segmentation techniques, therefore all the sample points have to be densely spaced, i.e., many segments need to be used. Third, segmentation techniques increase the size of the circuit matrix; the interdependence between the unknown internal variables at the present time-point requires their simultaneous solution. This is not the case in the state-based method, where the new state at any internal point is calculated individually and explicitly.

An understanding of why convolution is quadratic time while the state-based method is linear time, although both are equivalent if truncation and roundoff errors are not considered, can be obtained by considering what data is used by each method to recreate the line's past activity. The physical nature of the problem makes it possible for all the information needed for future simulation to be represented as the functions $v_0(\cdot)$ and $i_0(\cdot)$ over the fixed interval $[0,l]$. In convolution, this information is obtained indirectly from the values of the port variables over the interval $[0,t]$. This is inefficient, for this interval becomes increasingly less compact as the simulation proceeds.

The main computational effort in the state-based method is the calculation of the new line state at every time-point. The computation involved is however approximately independent of time, depending only on the number of internal samples of the line[7]; hence the linear complexity, which implies that for simulation lengths generating more than some N_{crit} time-points, the state-based method is faster than the convolution method. The crucial question is, of course, whether N_{crit} is achieved and exceeded in practical simulations. Examples in Section VI show that this is so in realistic circuits being simulated for one or more clock or data pulses.

The computation of the expressions in (31)–(35) dominates the execution time taken by the state-based method. In the implementation reported in this paper, these functions are calculated without any computation-reducing approximations. The nature of the functions is smooth, however, so pre-

[7]Given a dynamic sample point allocation scheme (see Section V), the number of internal samples needed is proportional to the "activity" of the waveforms inside the line.

calculation and using table-based lookups or spline approximations is expected to provide significant speedup without appreciable loss of accuracy.

V. Implementation Issues

The techniques described in the preceding section have been implemented in an experimental version of the circuit simulator SPICE 3, version 3e.1 [22].

The one-step convolution in the LHS of (36)–(39) is performed using the first term of the numerical convolution technique described in Section II. The evaluation of the integral in (35) is not computationally demanding, except when large time-steps are taken by the simulator; one Runge–Kutta step usually provides adequate accuracy. The implementation provides the option of choosing from different integration techniques (Runge–Kutta, Simpson, Burlisch–Stoer, Trapezoidal).

In the current implementation, the sample points for the line's internal state are dynamically determined by a simple and conservative heuristic method. The fact that waves propagate into the line from both ends is exploited. A list of sample points for the wave propagating from the left end is maintained; at every new time-step, the points are shifted to the right by the distance $\frac{t}{\gamma_0}$ travelled by the wave. This list is merged with a symmetric set of points from the right end of the line to obtain the complete set of sample points for the current time-point. At the start of the simulation, the merged list contains only the two end-points of the line; by the above procedure, the sequence of time-steps selected by the simulator completely determines the dynamic list of internal sample points. Some computation is saved because the merged set is symmetric about the center of the line. This simple dynamic sampling scheme is over-conservative, since lines in "quiet" sections of the circuit have their sample points determined by the same simulator time-step that determines the samples of lines in more "active" parts of the circuit. Experimentation is currently under way with dynamic sample point allocation schemes that take full advantage of the state-based technique by automatically exploiting latency.

VI. Experimental Results

Waveform and computation speed comparisons with the lumped-RLC and convolution methods for four circuits are presented in this section.

The first three circuits use BJT digital drivers with output rise-times of 500 ps–2 ns, connected by lossy interconnect to diode receivers or other BJT drivers. **raytheon1** has one fan-out, **raytheon2** has branching interconnect to three fan-outs and **raytheon3** has a 2-wire multiconductor line; all three use identical interconnect parameters[8]. **mosaic** is a single lossy line driven by a voltage source with series resistance and terminated by clamping diodes; interconnect parameters for **mosaic** were taken from [23]. For the lumped-RLC method, 240 segments were used for the first three circuits, and 64 segments for **mosaic**.

It is seen from Table II that the state-based method is more efficient than the convolution and lumped-RLC methods for the longer simulations, with speedups of more than 10 and 50, respectively. The convolution method itself is more than 5–10 times faster than the lumped-RLC method for the shorter simulations. Fig. 1 shows the variation of execution time for the three methods as the simulation length is increased.

[8] These circuits were provided by Raytheon Co.

TABLE II
Comparison Of Execution Times

Circuit	Simulation Length (ns)	Execution Time (s)		
		lumped-RLC	Convolution	State-Based
raytheon1	60	739	19.43	20
	120	1550	62.31	41.3
	180	2237	131.32	60
	240	3002	220	78
raytheon2	60	336.35	37	28.7
	120	668.3	110	52
	180	1027	239	78.7
	240	1372	380	99.6
	1000	5646	6301	428
raytheon3	60	885	40	28
	120	1791	141	57
	180	2700	529.41	95.3
mosaic	10	44.44	0.9	2
	20	93.18	3.6	2
	40	181.3	12.9	3.5
	80	371	49.5	6

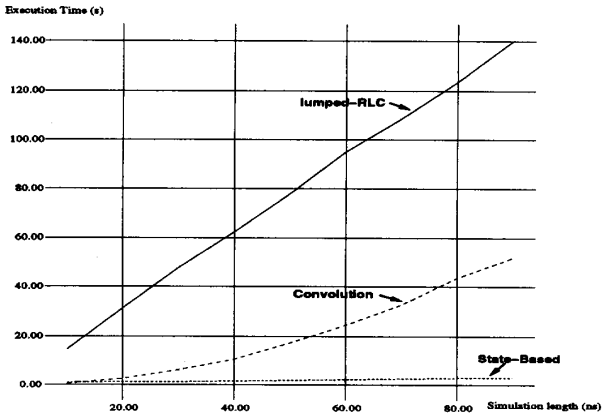

Fig. 1. **mosaic:** execution time versus simulation length.

The relative accuracies of the three methods can be compared visually in Figs. 2–5. For the **raytheon** circuits, the lumped-RLC method is as accurate as the other two, due to the large number of segments used for modelling the lines. In the **mosaic** circuit (Fig. 5), spurious ringing, characteristic of the lumped-RLC method, can be seen.

VII. Conclusion

A new linear time technique for simulating simple lossy transmission lines has been presented. The technique uses exact analytic forms for impulse responses and related functions. The key principle of the technique is to incorporate information about the internal state of the line into an analytic solution of the Telegrapher Equations. Dynamic allocation of

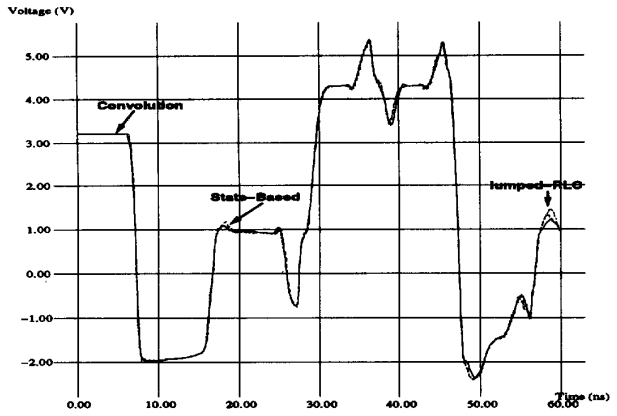

Fig. 2. **raytheon1** receiver-end voltage.

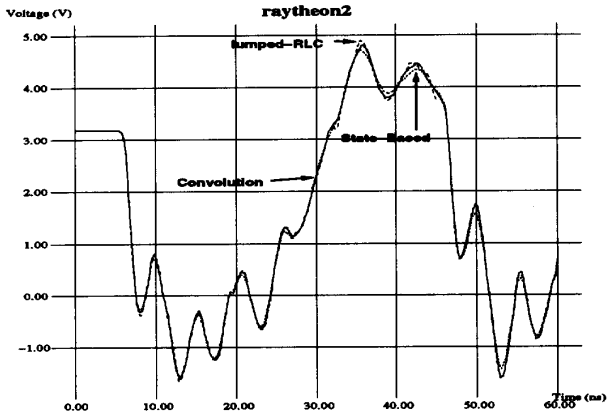

Fig. 3. **raytheon2**, voltage at one receiver.

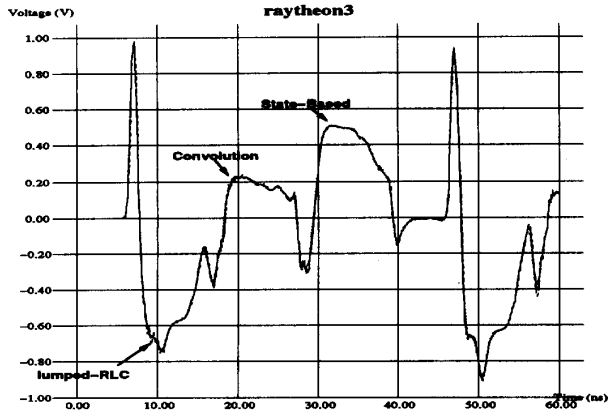

Fig. 4. **raytheon3, far-end crosstalk.**

state sample points is possible for automatic exploitation of latency. Analytic forms for impulse responses have also been applied to the existing convolution method, removing the need for numerical inversion. Generalizations of the Trapezoidal and Euler methods have been presented for numerical convolution that take advantage of the analytic forms. Experimental simulations verify the linear complexity of the state-based technique, demonstrating significant speedup over the convolution and lumped-RLC methods. In addition, convolution using the analytic responses and numerical formulae of this work is seen to be superior in accuracy to the lumped-RLC method while being significantly faster for short simulations.

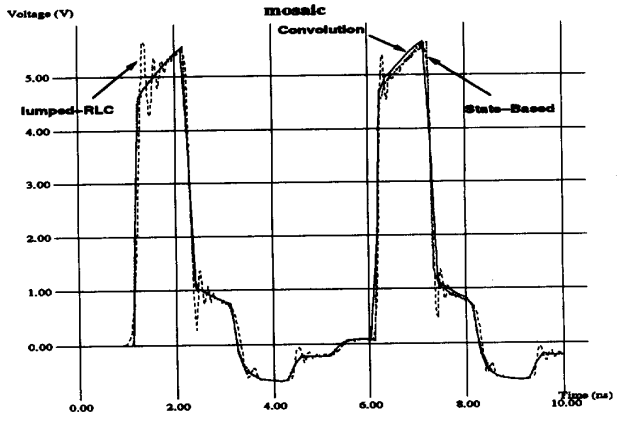

Fig. 5. **mosaic** receiver-end voltage.

VIII. Appendix A

A. Generalized Trapezoidal Method

In order to generalize the Trapezoidal method for the numerical convolution of (40), the assumption is made that $x(t)$ is piecewise linear, i.e., of the following form:

$$x(t) = x_i + m_i(t - t_i), t \in [t_i, t_{i+1}), i = 0, \ldots, n-1 \quad (49)$$

Using (49), (40) is split up into a sum of integrals over the piecewise linear regions and expressed as:

$$y(t_n) = \sum_{i=0}^{n-1} \int_{t_i}^{t_{i+1}} (x_i + m_i(\tau - t_i))h(t_n - \tau)d\tau \quad (50)$$

Equation (50) is evaluated by parts and algebraically manipulated to arrive at the following:

$$\begin{aligned} y_n = {} & x_n \frac{F(h, t_n - t_{n-1})}{t_n - t_{n-1}} \\ & + \sum_{i=1}^{n-1} x_i \left[\frac{F(h, t_n - t_{i-1}) - F(h, t_n - t_i)}{t_i - t_{i-1}} \right. \\ & \left. - \frac{F(h, t_n - t_i) - F(h, t_n - t_{i+1})}{t_{i+1} - t_i} \right] \\ & + x_0 \left[E(h, t_n - 0) - \frac{F(h, t_n - 0) - F(h, t_n - t_1)}{t_1 - 0} \right] \end{aligned} \quad (51)$$

where

$$E(h,t) \triangleq \int_0^t h(\tau)d\tau \quad (52)$$

$$F(h,t) \triangleq \int_0^t \int_0^\tau h(\tau')d\tau' d\tau \quad (53)$$

If $x_0 = 0$[9], the last term in (51) drops out:

$$y_n = x_n \frac{F(h, t_n - t_{n-1})}{t_n - t_{n-1}} + \sum_{i=1}^{n-1} x_i \left[\frac{F(h, t_n - t_{i-1}) - F(h, t_n - t_i)}{t_i - t_{i-1}} - \frac{F(h, t_n - t_i) - F(h, t_n - t_{i+1})}{t_{i+1} - t_i} \right] \quad (54)$$

which is the numerical integration formula (41).

B. Local Truncation Error

If $x(t)$ is not piecewise linear, define the error ϵ_n and the local error $\Delta\epsilon_n$ as follows:

$$\epsilon_n \triangleq y_n - \int_0^{t_n} x(\tau) h(t_n - \tau) d\tau \quad (55)$$

$$\Delta\epsilon_n \triangleq \epsilon_n - \epsilon_{n-1} \quad (56)$$

By an analysis analogous to that for differential equations [21], the following expression can be obtained for the local error:

$$\begin{aligned} \Delta\epsilon_n = {} & x''(\tau_n^*) \left\{ \frac{F(h, t_n - t_{n-1})(t_n - t_{n-1})}{2} - G(h, t_n - t_{n-1}) \right\} \\ & + \sum_{i=1}^{n-1} x''(\tau_i^*) \left[\frac{(t_i - t_{i-1})}{2} \{ F(h, t_n - t_{i-1}) + F(h, t_n - t_i) \right. \\ & - F(h, t_{n-1} - t_{i-1}) - F(h, t_{n-1} - t_i) \} \\ & + G(h, t_n - t_i) - G(h, t_n - t_{i-1}) \\ & \left. - G(h, t_{n-1} - t_i) + G(h, t_{n-1} - t_{i-1}) \right] \end{aligned} \quad (57)$$

where

$$G(h, t) \triangleq \int_0^t \int_0^\tau \int_0^{\tau'} h(\tau'') d\tau'' d\tau' d\tau \quad (58)$$

$x''(\cdot)$ refers to the second derivative of $x(t)$, and $\tau_i^* \in [t_{i-1}, t_i]$, $i \in \{1, \ldots, n\}$.

If $h(\tau) \equiv 1$, then $F(t) = \frac{t^2}{2}$, $G(t) = \frac{t^3}{6}$. If these are substituted into (57), it can be shown after algebraic manipulation that the coefficients of $x''(\tau_i^*)$ inside the $\sum$ become identically zero, and the expression reduces to the first term which simplifies to $x''(\tau_n^*) \frac{(t_n - t_{n-1})^3}{12}$, the local truncation error estimate for the trapezoidal method.

IX. Appendix B

A. Dealing with a Nonzero Initial dc Condition

Assume there exist two sets of solutions $(v^a(x,t), i^a(x,t))$ and $(v^b(x,t), i^b(x,t))$ to (1) and (2). Since the Telegrapher Equations are *linear* PDE's, any linear combination of the above solutions (with coefficients not involving x or t) is also a solution of the Telegrapher Equations. The dc solution $(v^{dc}(x), i^{dc}(x))$ is a particular solution of the Telegrapher Equations. Therefore, given any other solution $(v(x,t), i(x,t))$, the linear combination $(v^\dagger(x,t), i^\dagger(x,t))$, where $v^\dagger(x,t) = v(x,t) - v^{dc}(x)$, $i^\dagger(x,t) = i(x,t) - i^{dc}(x)$, satisfies the Telegrapher Equations.

[9]This can be assumed without loss of generality; see Appendix B.

Therefore, v and i can be replaced by $v^\dagger$ and $i^\dagger$ in all the equations in Section II. Thus, if the simulation starts from a dc steady-state, then $v^\dagger(x,0) = i^\dagger(x,0) = 0$.

Acknowledgment

The encouragement and support provided by Gerry Marino is greatly appreciated. Discussions with Albert Ruehli, Kishore Singhal and Jacob White were very helpful. Thanks are due to Sally Liu and Peter Lloyd for encouragement and support.

References

[1] L.-T. Hwang, *et al.*, "The Effects of the Skin-Depth on the Design of a Thin-Film Package," MCNC, Research Triangle Park, NC.

[2] A. R. Djordjević and T. K. Sarkar, "Analysis of time response of lossy multiconductor transmission line networks," *IEEE Trans. Microwave Theory Techniq.*, vol. MTT-35, pg. 898, Oct. 1987.

[3] E. Lelarasmee, A. E. Ruehli, and A. L. Sangiovanni-Vincentelli, "The wavefrom relaxation method for time domain analysis of large scale integrated circuits," *IEEE Trans. Computer-Aided Design*, vol. CAD-1, pp. 131–145, July 1982.

[4] J. K. White and A. Sangiovanni-Vincentelli, *Relaxation Techniques for the Simulation of VLSI Circuits*. Boston, MA: Kluwer, 1987.

[5] F. Y. Chang, "Relaxation simulation of transverse electromagnetic wave propagation in coupled transmission lines,"*IEEE Trans. Circ. Sys.*, vol. 38, pp. 916–936, Aug. 1991.

[6] R. Wang and O. Wing, "Analysis of VLSI multiconductor systems by bi-level waveform relaxation," in *Proc. ICCAD*, 1190, pp. 166–169.

[7] K. Singhal and J. Vlach, "Computation of time domain response by numerical inversion of the laplace transform," *J. Franklin Inst.*, vol. 299, no. 2, pp. 109–126, Feb. 1975.

[8] H. W. Dommel, "Digital computer solution of electromagnetic transients in single and multiphase networks," *IEEE Trans. Power App. Sys.*, vol. PAS–88, pg. 388, Apr. 1969.

[9] A. J. Gruodis and C. S. Chang, "Coupled lossy transmission line characterization and simulation," *IBM J. Res. Dev.*, Jan. 1981.

[10] L. T. Pillage and R. A. Rohrer, "Asymptotic waveform evaluation for timing analysis," *IEEE Trans. Computer-Aided Design*, vol. 9, pp. 352–366, Apr. 1990.

[11] X. Huang, V. Raghavan, and R. A. Rohrer, "AWEsim: A program for the efficient analysis of linear(ized) circuits," in *Proc. ICCAD*, Nov. 1990, pp. 534–537.

[12] S. Lin and E. S. Kuh, "Padé approximation applied to transient simulation of lossy coupled transmission lines," in *Proc. IEEE Multi-Chip Module Conf.*, Santa Cruz, CA, Mar. 1992.

[13] T. K. Tang, M. S. Nakhla, and R. Griffith, "Analysis of lossy multiconductor transmission lines using the asymptotic waveform evaluation technique," *IEEE Trans. Microwave Theory Techniq.*, vol. 39, pp. 2107–2116, Dec. 1991.

[14] J. E. Bracken, V. Raghavan, and R. A. Rohrer, "Extension of the asymptotic waveform evaluation technique with the method of characteristics," in *Proc. ICCAD*, Nov. 1992.

[15] C. Gordon, T. Blazeck, and R. Mittra, "Time domain simulation of multiconductor transmission lines with frequency-dependent losses," *IEEE Trans. Computer-Aided Design*, vol. 11, pp. 1372–1387, Nov. 1992.

[16] A. R. Djordjević *et al.*, "Analysis of lossy transmission lines with arbitrary nonlinear terminal networks,"*IEEE Trans. Microwave Theory Techniq.*, vol. MTT-34, pg. 660, June 1986.

[17] J. E. Schutt-Aine and R. Mittra, "Scattering parameter transient analysis of transmission lines loaded with nonlinear terminations," *IEEE Trans. Microwave Theory Techniq.*, vol. MTT-36, pp. 529–536, 1988.

[18] A. Deutsch, *et al.*, "High-speed signal propagation on lossy transmission lines," *IBM J. Res. Dev.*, vol. 34, no. 4, pp. 601–615, July 1990.

[19] Erwin Kreyszig, *Advanced Engineering Mathematics*. New Dehli, India: Wiley Eastern, 1985.

[20] G. Fodor, *Laplace Transforms in Engineering*. Budapest, Hungary: Akademiai Kiado, 1965.

[21] L. O. Chua and P.-M. Lin, *Computer-Aided Analysis of Electronic Circuits: Algorithms and Computational Techniques*. Englewood Cliffs, NJ: Prentice-Hall, 1975.

[22] T. L. Quarles, "Analysis of Performance and Convergence Issues for Circuit Simulation," Ph.D. dissertation, Memo. UCB/ERL M89/42, Elec. Res. Lab., EECS Dept., Univ. of California, Berkeley, CA, Apr. 1989.

[23] C. A. Neugebauer, *et al.*, High performance interconnections between VLSI chips, *Solid State Tech.*, June 1988.

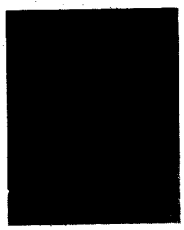

Jaijeet S. Roychowdhury received the B. Tech. degree in electrical engineering from the Indian Institute of Technology, Kampur, in 1987, and the M. S. and Ph. D. degrees in electrical engineering from the University of California at Berkeley in 1989 and 1993, respectively.

He is currently with the CAD Laboratory of AT&T Bell Laboratories, Allentown, PA.

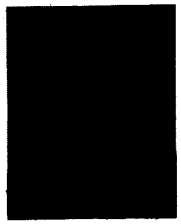

A. Richard Newton (S'73–M'78–SM'86–F'88) received the B. Eng. (elect.) and M. Eng. Sci. degrees from the University of Melbourne, Melbourne, Australia, in 1973 and 1975, respectively, and the Ph. D. degree from the University of California, Berkeley, in 1978.

He is currently a Professor and Vice Chairman of the Department of Electrical Engineering and Computer Sciences, University of California, Berkeley. He was the Technical Program Chairman of the 1988 ACM/IEEE Design Automation Conferences, and a consultant to a number of companies for computer-aided design of integrated circuits. His research interests include all aspects of the computer-aided design of integrated circuits, with emphasis on simulation, automated layout techniques, and design methods for VLSI integrated circuits.

Dr. Newton was selected in 1987 as the national recipient of the C. Holmes McDonald Outstanding Young Professor Award of Eta Kappa Nu. He is a member of Sigma Xi.

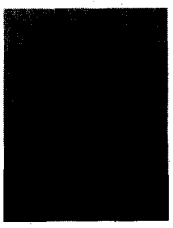

Donald O. Pederson (S'49–A'51–M'56–F'64–LF'91) received the B. S. degree from North Dakota State University in 1948 and the M. S. and Ph. D. degrees from Stanford University in 1949 and 1951. He was awarded an honorary Doctor of Applied Science by Katholieke Universiteit, Leuven, Belgium, in 1979. In 1991, he received the Berkeley Citation.

From 1951 to 1953 he was with the Electronics Research Laboratory, Stanford University, and from 1953 to 1955 with the Bell Telephone Laboratories, Inc. In 1955, he joined the University of California, Berkeley. He is now Professor Emeritus in the Department of Electrical Engineering and Computer Sciences, still engaged in teaching and research in the computer-aided design of microelectronic circuits. From 1960 to 1964 he was Director of the Electronics Research Laboratory. From 1983 to 1985 he was Chairman of the Department. From 1988 to 1991, he was the E. L. and H. H. Buttner Professor of Electrical Engineering.

Dr. Pederson was appointed a Distinguished Fulbright Lecturer to Ireland in 1988. He is a Fellow of the American Academy of Arts and Sciences (1991) and was a 1964 Guggenheim Fellow. He was the recipient of the 1969 IEEE Educational Medal, of the IEEE Centennial Medal (1984), and, in 1985, of the IEEE Solid-State Circuit Council's Outstanding Development Award. In 1974, he was elected to the National Academy of Engineering, and in 1982 to the National Academy of Sciences. He is a member of the Board of Directors of Tektronix, Inc., of Valid Logic Systems, Inc., and of Varian Associates, Inc.